



International Conference on Industry 4.0 and Smart Manufacturing

Improvement of manufacturing technologies through a modelling approach: an air-steam sterilization case-study

Francesca Iacono^a, Jorge Lo Presti^a, Irene Schimperia^a, Sara Ferretti^b, Andrea Mezzadra^b, Lalo Magni^c, Chiara Toffanin^{a,*}

^aDepartment of Electrical, Computer and Biomedical Engineering, University of Pavia, via Ferrata 3, Pavia, 27100, Italy

^bFedegari Autoclavi SpA, SS 235 km 8, Albuzzano (PV), 27010, Italy

^cDepartment of Civil and Architecture Engineering, University of Pavia, via Ferrata 3, Pavia, 27100, Italy

Abstract

A milestone of Industry 4.0 is the improvement of the design procedures requiring models of complex processes. Models can be used to simulate the process, being accurate even if complex, and to predict process behaviour for control action, requiring simplicity and stability. In the last years, machine learning approaches came up alongside of the standard identification techniques for prediction purposes. In this work we propose two models of an industrial autoclave to describe the evolution of temperature and pressure. The first model (PhM) involves a physical structure with data-driven adaptation of the parameters, the second one is a Long Short-Term Memory network (LSTM), trained ensuring Input-to-State stability. Both models obtained good performance: FIT of 94.26% (91.55%) for the temperature (pressure) with PhM; 84.59% (78.31%) for the temperature (pressure) with the LSTM. Future developments involve the synthesis of an MPC based on the LSTM to be tested in simulation via PhM.

© 2021 The Authors. Published by Elsevier B.V.

This is an open access article under the CC BY-NC-ND license (<https://creativecommons.org/licenses/by-nc-nd/4.0>)

Peer-review under responsibility of the scientific committee of the International Conference on Industry 4.0 and Smart Manufacturing

Keywords: Modelling; Identification; Model validation; Neural Network

1. Introduction

In order to meet the principles of Industry 4.0, the modelling of complex processes is required and, thanks to the availability of a large amount of data, this goal is now achievable. An interesting case study is represented by the autoclaves, pressurized chambers used for the sterilization through the control of temperature and pressure, when high temperatures and pressures other than ambient ones are required. In this work an air-steam sterilizer is considered, where the sterilization is performed using a mix of air and steam, in order to balance the pressure inside the machine through air injection while reaching the sterilization temperature target through steam injection. The presence of

* Corresponding author. Tel.: +39-0382-985354.

E-mail address: chiara.toffanin@unipv.it

multiple outputs and control variables, interacting with each other, complicates the process making its modelling not trivial. Moreover, the use of these machines in different fields of applications leads to a large variety of autoclaves available on the market with different size, toolkits, and components, and so different models are necessary. However, even if each machine requires a specific physical model, starting from a common basic model representing the main processes occurring in an autoclave, the new model can be obtained adapting the basic one to the specific case.

Previously, few works in the literature faced this modelling problem: in each case, the proposed model was specific of the analysed process and could not be easily adapted to others. For example, in [11] an autoclave for curing of composites, and in [2] one for chemical leaching process were proposed; the heat transfer between the autoclave and the product was analysed in [14], [8]. A purely physical approach to a similar problem was proposed in [13] showing a not optimal results for this kind of processes. Despite the affinities with some of these machines, the differences in the processes considered here require a new model.

In this work, two models of an industrial air-steam sterilizer are proposed. The first one is a physical model, to be used for simulation, obtained from a previous model of a lab equipment sterilizer proposed in [6]. The second model exploits neural network techniques, through the training of a particular Recurrent Neural Network (RNN), to obtain a model for control applications. In the latter case also the stability properties of the system are investigated.

The first model is the result of a hybrid approach, similar to the one proposed in [6], that involves a physical structure with data-driven adaptation of the parameters. In this way, the parameters take into account the model uncertainties derived by the physical modelling, while the main structure is based on the physical laws that affect the temperature and pressure behaviours. This model allows to simulate the effect of possible design changes before applying them. The second solution is a black-box approach, where a RNN is used to identify the system. This approach requires a greater amount of data but provides in short time a good model of the machine on which the data were acquired. Moreover, the stability property of this network can be ensured applying a constrained training process, so the model can be used inside model-based controllers.

Both solutions have been tested on data provided by Fedegari Group (Albuzzano, Italy), a company specialised in the production of autoclaves, particularly sensitive to the topic of Industry 4.0. The two models showed satisfactory results.

The manuscript is organised as follows: in Section 2 the autoclave and the air-steam cycle analysed in this work are described; in Section 3 the physical model (PhM) is presented in details and in Section 4 the neural network model is introduced together with its stability property. A brief discussion is presented in Section 5 analysing pro and cons of each solution and the conclusions are drawn in Section 6.

2. Autoclave description

An autoclave is a pressurized chamber used to sterilize different products, exploiting pressurized steam. In this work, an industrial autoclave with internal heat exchangers (plates) and a jacket surrounding the chamber, to pre-heat and cool down the chamber through steam and cold water, is studied. Inside the chamber a fan to distribute homogeneously air and steam is also present.

2.1. Air-steam cycle

The machine considered in this work can perform sterilization cycles using a mixture of air and steam, typical for the sterilization of liquid in sealed containers. Under these conditions, when the product is heated up, the liquid expands, exerting pressure. Consequently the pressure inside the chamber has to balance the liquid one, through the regulation of air and steam as described in [12]. The cycle is composed by four different phases, shown in Fig. 1, where an example of temperature and pressure profiles is reported. The cycle starts with the preparation of the autoclave (Ph1) during which the initial conditions are set and checked. Then, the chamber is heated (Ph2) injecting steam in the chamber with the possibility of activating auxiliary elements (plates and jacket) to speed up the process. This phase lasts until target temperature and pressure are reached and they are maintained throughout the sterilization phase (Ph3). At the end of the sterilization, the cooling phase starts. Firstly, there is a pressurization using only compressed air (Ph4) and then a controlled rate cooling (Ph5) during which the auxiliary elements can be activated to cool down the chamber.

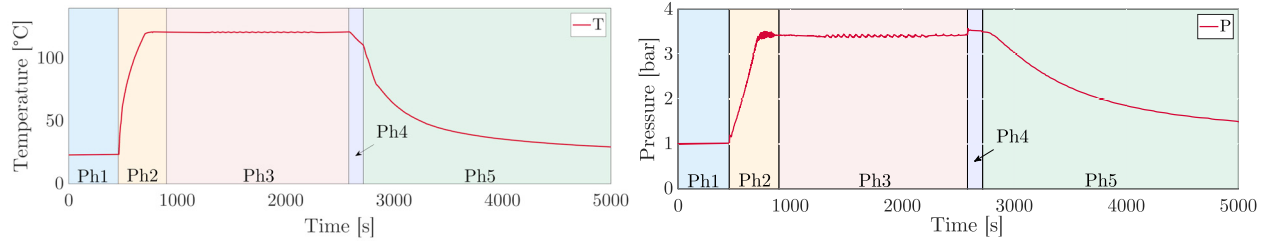


Fig. 1: Temperature (left) and pressure (right) profiles during the air-steam cycle.

3. Physical model for simulation

In this Section the physical model (PhM) obtained extending the previous model of a lab equipment sterilizer [6] is presented.

The sterilization process can be described through the definition of five different processes: i) chamber filling and emptying; ii) chamber pressure regulation; iii) chamber heating and cooling; iv) plates heating and cooling; v) jacket heating and cooling. Processes i)-iii) were already present in [6] and will be integrated here with the effect of plates and jacket. The outputs of the system are the pressure and the temperature of the chamber. The temperature of the jacket is also measured and can be a variable of interest, so an additional output has been introduced in the model. A discrete state is added to take into account different conditions of the chamber, that imply different physical laws for temperature and pressure.

3.1. Description

The dynamic of the system is described by seven states:

- $x_1(t) = Q_a(t)$ air quantity in the chamber;
- $x_2(t) = Q_s(t)$ steam quantity in the chamber;
- $x_3(t) = P_c(t)$ chamber pressure;
- $x_4(t) = T_c(t)$ chamber temperature;
- $x_5(t) = T_p(t)$ plates temperature;
- $x_6(t) = T_j(t)$ jacket temperature;
- $x_7(k) = CC(k)$ chamber conditions.

The discrete state $x_7(k)$ depends on the values of $x_1(t)$ and $x_2(t)$. In fact, temperature and pressure follow different physical laws, based on the quantities of air and steam inside the chamber. For this reason, the finite state machine proposed in [6] is still valid. It is used to determine the different chamber condition between:

- Vacuum (V): no gas in the chamber ($x_7(k) = 0$);
- Mixed (M): both air and steam in the chamber ($x_7(k) = 1$);
- Saturated steam (S): only steam in the chamber ($x_7(k) = 2$);
- Air (A): only air in the chamber ($x_7(k) = 3$).

In the air-steam cycle only mixed ($x_1(k), x_2(k) > 0$) and air ($x_1(k) > 0, x_2(k) = 0$) cases are verified.

The chamber, plates and jacket inputs are reported in Table 1. In this work, the presence of valves that can work as on/off or as modulated valves is considered. In particular, their working mode is regulated by the activations, a_v and a_w , of the analogue signals v and w , respectively. These signals modulate the opening of the valves: when the signals is active ($a_v = 1, a_w = 1$) the valves are modulated, otherwise they are in the on/off mode and their state is determined by the activation state a_n of the specific valve n . Inputs $u_1(t)$, $u_2(t)$, $u_4(t)$, $u_5(t)$ and $u_{11}(t)$ depend on the signal v , input $u_8(t)$ depends on the signal w , following a non linear relation that is approximated in this work with a sigmoid function. When they control an input flow (steam, air or cooling water), the valve is completely open when the signal is high. Vice versa, when they control a drain, the valve is completely open when the signal is low. In this way it is possible to control two opposite effects with a unique signal.

In the following, when a valve n is modulated, its input is indicated as u_n , while when it functions as on/off, its input

Table 1: Inputs used in the PhM reported as the variable name used in the equations (input), the name of the variable (signal) and a short description. The variables are grouped in three parts (chamber, plates and jacket) to highlight where the inputs act.

	Input	Signal	Description
Chamber	$u_1(t)$	$Q_{ca}(t)$	ingoing compressed air flow
	$u_2(t)$	$Q_{st}(t)$	ingoing steam flow
	$u_3(t)$	$a_f(t)$	fan activation state (0,1)
	$u_4(t)$	$d_1(t)$	drain 1 contact surface
	$u_5(t)$	$d_2(t)$	drain 2 contact surface
	$u_6(t)$	$d_3(t)$	drain 3 activation state
Plates	$u_7(t)$	$Q_{st,p}(t)$	ingoing steam flow in the plates
	$u_8(t)$	$Q_{H_2O,p}(t)$	ingoing water flow in the plates
	$u_9(t)$	$d_4(t)$	drain 4 activation state
Jacket	$u_{10}(t)$	$Q_{st,c}(t)$	ingoing steam flow in the jacket
	$u_{11}(t)$	$Q_{H_2O,c}(t)$	ingoing water flow in the jacket
	$u_{12}(t)$	$d_5(t)$	drain 5 activation state
	$u_{13}(t)$	$d_6(t)$	drain 6 activation state
	$u_{14}(t)$	$d_7(t)$	drain 7 activation state

is indicated as a_n , referring to the activation of the valve.

If different valves are used to control the ingoing/outgoing flows, it is possible to adapt the model studying the new component and changing the expression of $u_n(t)$.

The final equations of the proposed model are presented in the following. The first two states represent the quantities of the gases present in the chamber:

$$\begin{aligned} \dot{x}_1(t) &= u_1(t) - k_{d_1}u_4(t)(x_3(t) - P_a)P_{or} \cdot \left(1 - \frac{x_2(t)}{x_1(t)+x_2(t)}u_3(t)\right)q_a - k_{d_2}u_5(t)(x_3(t) - P_a)P_{or} \cdot \left(1 - \frac{x_2(t)}{x_1(t)+x_2(t)}u_3(t)\right)q_a \quad (1) \\ \dot{x}_2(t) &= u_2(t) - k_{d_1}u_4(t)(x_3(t) - P_a)\frac{x_2(t)}{x_1(t)+x_2(t)}P_{or} \cdot (1 - q_a(1 - u_3(t)))q_s \\ &\quad - k_{d_2}u_5(t)(x_3(t) - P_a)\frac{x_2(t)}{x_1(t)+x_2(t)}P_{or}d \cdot (1 - q_a(1 - u_3(t)))q_s - k_1(x_4(t) - T_a)q_sT_{or} \end{aligned}$$

where P_{or} (T_{or}) is an auxiliary logic variable active if the pressure x_3 (temperature x_4) is above the threshold P_a (T_a), while q_a and q_s detect the presence of air ($x_1(t) > 0$) and steam ($x_2(t) > 0$), respectively.

The quantities x_1, x_2 depend on the ingoing flow of compressed air, $u_1(t)$, or steam, $u_2(t)$, and on the outgoing flow through the chamber drains, $u_4(t)$ and $u_5(t)$. The outgoing flow is proportional to the difference between the pressure inside the chamber and the atmospheric one, P_a , if the pressure inside is greater than it. The machine is equipped with a fan, $u_3(t)$, in order to have an homogeneous distribution of gases inside the chamber. If the fan is active, the two gases will be expelled proportionally to their quantities in the chamber, otherwise the air will be expelled firstly because the drains are located on the bottom. A term to take into account the condensation effect of the steam is also added in Eq. (1).

The third state describes the pressure evolution and depends on the chamber condition. In the Mixed case ($x_7 = 1$) the pressure equation is:

$$\dot{x}_3(t) = + k_{p,u_{1m}}u_1(t)(x_3(t) - P_a) + k_{p,u_1}u_1(t)(x_4(t) - T_a) - k_{p,d_{2m}}u_5(t)(x_3(t) - P_a) - k_{p_m}(x_3(t) - P_{st}(x_4(t))) \quad (2)$$

So, it increases due to the injection of compressed air and decreases because of the opening of the drains. A condensation effect is present due to the injection of air with a lower temperature (atmospheric one, T_a) with respect to the temperature of the gas inside the chamber. The fourth term of Eq. (5) represents the one-to-one correspondence between temperature in Kelvin (T_c^k) and pressure (P_{st}) inside the chamber: $P_{st}(T_c^k(t)) = f(T_c^k(t)) = P_{wv}(T_c^k(t)) + P_{as}(T_c^k(t))$ where P_{wv} is given by water vapour pressure law [4]

$$P_{wv}(T_c^k(t)) = \frac{e^{\frac{73.649 - \frac{7258.2}{T_c^k(t)} + 4.1653 \cdot 10^{-6} \cdot T_c^k(t)^2}}{e^{7.3037} \cdot T_c^k(t)} \quad (3)$$

and P_{as} is proportional to the temperature T_c^k following the law related to the overpressure inside sealed container with aqueous solution [12]. Note that a similar relation stands in the saturated steam case so that Eq. (2) can be easily adapted to that new case. In the Air case ($x_7 = 3$) we obtain:

$$\begin{aligned} \dot{x}_3(t) = & + k_{p,u1}u_1(t)(x_3(t) - P_a) - k_{p,d1}u_4(t)(x_3(t) - P_a) - k_{p,d2}u_5(t)(x_3(t) - P_a) \\ & - k_{p,cool_{pl}}a_8(t)(x_3(t) - P_a) - k_{p,cool_j}a_{11}(t)(x_3(t) - P_a) \end{aligned} \quad (4)$$

The pressure of the chamber is increased by the injection of compressed air and is decreased by the activation of drain 1, $u_4(t)$, or drain 2, $u_5(t)$. There is a further decreasing when jacket and/or plates are filled with cooling fluid.

The fourth state represents the temperature inside the chamber, and as the pressure, it depends on the chamber conditions. In the Mixed case ($x_7 = 1$) the temperature is:

$$\begin{aligned} \dot{x}_4(t) = & + k_{c,u_{2m}}(T_{ot0})u_2(t)(T_{stmax} - x_4(t)) - k_{c,d_{2m}}u_5(t)(x_4(t) - T_a) \\ & - k_{c,d_3}a_6(t)(x_4(t) - T_a) + k_{c,pl_m}a_7(t)(x_5(t) - x_4(t)) \end{aligned} \quad (5)$$

So, it increases due to the injection of steam until T_{stmax} is reached, that is the maximum temperature that can be reached through steam injection. It is decreased by the opening of drains 1 and 3. An heat exchange between chamber and plates increases or decreases the temperature, proportionally to the temperature difference of the two elements. Note that, the parameter $k_{c,u_{2m}}$ depends on the initial temperature of the chamber $x_4(0)$; in particular, T_{ot0} is an auxiliary logic variable active if the initial temperature is above the threshold $T_{th} = 30^\circ$. In the Air case ($x_7 = 3$) we obtain:

$$\begin{aligned} \dot{x}_4(t) = & - k_{c,d_1}u_4(t)(x_4(t) - T_a) - k_{c,d_2}u_5(t)(x_4(t) - T_a) - k_{c,u_1}u_1(t)(x_4(t) - T_a) - k_{c,d_{1pl}}(a_4(t) + a_8(t))(x_4(t) - T_a) \\ & - k_{c,d_{2pl}}(a_5(t) + a_8(t))(x_4(t) - T_a) - k_{c,pl}a_8(t)(x_4(t) - T_p) - k_{c,j}a_{11}(t)(x_4(t) - T_a) \end{aligned} \quad (6)$$

where $k_{c,d_{1pl}} = \bar{k}_{c,d_{1pl}}$, $k_{c,d_{2pl}} = \bar{k}_{c,d_{2pl}}$ and $k_{c,pl} = 0$ in the interval $[\bar{t}_p, \bar{t}_p + \tau_1]$, and $k_{c,d_{1pl}} = k_{c,d_{2pl}} = 0$, $k_{c,pl} = \bar{k}_{c,pl}$ otherwise, with \bar{t}_p the time of the activation of the cooling fluid in the plates. The temperature is decreased by drain 1 or 2, the injection of compressed air and the cooling effect of the jacket. The cooling effect of the plates is also present. At the beginning, it depends on $k_{c,d_{1pl}}$ or $k_{c,d_{2pl}}$, after τ_1 it depends on $k_{c,pl}$ and tends to the plates temperature, T_p . This happens because after this time interval the cooling fluid of the plates has reached a thermal equilibrium with the chamber, so its cooling effect is slightly reduced.

The fifth state is the plates temperature:

$$\dot{x}_5(t) = + k_{pl,u_7}a_7(t)(T_{stmax} - x_5(t)) - k_{pl,d_4}a_9(t)(x_5(t) - T_a) - k_{pl,c}a_7(t)(x_5(t) - x_4(t)) \quad (7)$$

It is increased by the injection of steam in the plates through $u_7(t)$, until the sterilization temperature is reached, and decreased through the drain 4, $u_9(t)$, proportionally to the atmospheric temperature. The temperature of the plates also depends on the heat exchange with the chamber, proportionally to the temperature difference of the two elements.

The sixth state represents the jacket temperature.

$$\begin{aligned} \dot{x}_6(t) = & + k_{j,c}(x_4(t) - x_6(t)) + k_{j,u_2}u_2(t)(T_{steam} - x_6(t)) + k_{j,u_{10}}a_{10}(t - \tau_2)(T_{stmax} - x_6(t)) \\ & - k_{j,d_5}a_{12}(t)(x_6(t) - T_a) - k_{j,d_6}a_{13}(t)(x_6(t) - T_a) - k_{j,d_7}a_{14}(t)(x_6(t) - T_a) - k_{j,pl}a_8(t - \tau_1)(x_6(t) - T_a) \\ & - k_{j,cool}a_{11}(t - \tau_2)(x_6(t) - T_a) + k_{j,fl}a_{11}(t)(T_{steam} - x_6(t)) - k_{j,disp}a_{12}(t)(x_6(t) - T_{steam}) \end{aligned} \quad (8)$$

where $k_{j,fl} = \bar{k}_{j,fl}$ in the interval $[\bar{t}_c, \bar{t}_c + \tau_2]$ and zero otherwise, with \bar{t}_c the time of the activation of the cooling fluid in the jacket delayed by a constant α . In the interval $[\bar{t}_d, \bar{t}_d + \tau_3]$ we have $k_{j,disp} = \bar{k}_{j,disp}$ while it is zero otherwise, with \bar{t}_d the time of the activation of the drain 5.

Since the chamber is completely surrounded by the jacket, there is always an heat exchange between them. The temperature of the jacket increases when steam is injected inside the chamber through $u_2(t)$ and when steam is directly injected through $u_{10}(t)$, until the sterilization temperature is reached, considering a delay τ_2 due to the waiting time for the complete filling of the jacket. It decreases through the drains ($u_{12}(t)$, $u_{13}(t)$, $u_{14}(t)$) and when the cooling fluid is present in the plates, $u_8(t)$, and in the jacket, $u_{11}(t)$, considering the delay τ_1 due to the waiting time for the cooling of the plates. The parameter $k_{j,fl}$ takes into account the delayed effect of the injection of cooling fluid in the jacket when the jacket is used for cooling. On the contrary, $k_{j,disp}$ considers the delayed effect of the drain 5 when the jacket is used for heating. All the delays reported in this section have been experimentally estimated.

Finally, the output transformation is given by: $y_1(t) = x_3(t)$, $y_2(t) = x_4(t)$, $y_3(t) = x_6(t)$.

Table 2: The available datasets are described with the main features that differentiate them: initial temperature (Low/High), auxiliary heating and cooling (None, Plates, Jacket, Plates&Jacket) and drain (1/2).

Run	Init. Temperature	Aux Heating	Aux Cooling	Drain
1	Low	None	Plates&Jacket	1
2	Low	None	Plates	1
3	Low	Plates	Plates&Jacket	1
4	Low	Plates	Plates	1
5	Low	Jacket	Plates	2
6	High	Plates	Plates&Jacket	1
7	High	Plates	Plates	1
8	High	Jacket	Plates	2
9	High	Jacket	Plates&Jacket	2
10	High	Plates&Jacket	Plates	1

3.2. Parameters estimation

The data used for the parameters estimation have been acquired on an industrial autoclave, kindly offered by Fedegari Autoclavi SpA, called in the following FHA (Fedegari Horizontal Autoclave). The high complexity of this machine and the optional use of the auxiliary components for the heating and cooling processes lead to several possible configurations of the sterilization cycle. In particular, they will be discriminated by: i) the initial temperature (high, low); ii) the auxiliary heating method (none, plates, jacket, both plates and jacket); iii) the cooling method (plates, both plates and jacket) and iv) the drain (1 or 2) used during the cooling phase. Of the total 32 possible configurations, ten datasets were collected on the FHA to cover most of the possible combinations, as shown in Table 2. In particular, the data collection was focused on obtaining at least all the possible combinations of the heating-cooling methods, in accordance with the company possibilities. The cycles using jacket and plates both in heating and cooling presented some problems during data collection and had to be excluded from this analysis.

The optimization procedure proposed in [6] required a collection of repeated datasets for each configuration of the considered air-steam cycle, that are not currently available for the FHA. So, in this work, the parameters tuning is performed via a trial and error procedure and the complete parameters optimization presented in [6] is demanded to a future work when further data collection of repeated tests will be acquired. In particular, a preliminary case-study is introduced here to validate the contributions of auxiliary heating and cooling components added to the previous state-space model.

3.3. Results

The tuning of the parameters was performed on half of the datasets present in Table 2, in particular on run 2, 3, 5, 6, 8. Then, the validation is performed on the other half (runs 1, 4, 7, 9, 10). The parameters specifically connected to the physical valves of the FHA have been set under the supervision of the technical staff of Fedegari company. In particular, the parameters of the sigmoid functions and the delays connected to the filling of plates and jacket are $\tau_1 = \tau_3 = 180s$, $\tau_2 = 120s$ and $\alpha = 60s$.

The goodness of fit [9] of the model is measured for temperature and pressure in the chamber. A complementary validation has been added with respect to [6] for the temperature in the jacket since the measure of this variable is available in the datasets (while no direct measure is possible for the plates) and it is one of the contributions of this work. The considered performance indexes are the index of fitting $FIT = 100 \left(1 - \frac{\|\hat{Y} - Y\|}{\|Y - \bar{Y}\|} \right)$ and the Pearson correlation

coefficient $\rho = \frac{\sum_{i=1}^n (Y_i - \bar{Y})(\hat{Y}_i - \bar{\hat{Y}})}{\|Y_i - \bar{Y}\| \|\hat{Y}_i - \bar{\hat{Y}}\|}$ where Y is the real values of the signal, \hat{Y} is the predicted ones, \bar{Y} is the mean of the real data and $\bar{\hat{Y}}$ is the mean of the predicted data. The results of the index calculation are shown in Table 3 (left) for temperature and pressure in the chamber, and for the temperature in the jacket. The mean of the performance indexes is reported in the last row of the table; these mean values will be referred as \overline{FIT} and $\overline{\rho}$.

Table 3: PhM results for chamber temperature and pressure and jacket temperature on the left. LSTM results for chamber temperature and pressure on the right.

Run	PhM						LSTM			
	Temperature		Pressure		Jacket		Temperature		Pressure	
	FIT	ρ	FIT	ρ	FIT	ρ	FIT	ρ	FIT	ρ
1	95.08	0.999	91.92	0.997	86.54	0.992	81.90	0.984	73.87	0.966
4	93.51	0.998	90.60	0.998	73.52	0.897	87.44	0.992	82.72	0.989
7	93.00	0.998	89.25	0.999	98.23	0.997	84.42	0.988	78.34	0.985
9	95.34	0.999	93.05	0.998	96.42	0.998	34.38	0.836	16.72	0.830
10	94.34	0.998	92.93	0.998	97.53	0.996	51.88	0.898	54.50	0.936
Av	94.26	0.998	91.55	0.998	90.45	0.976	84.59	0.988	78.31	0.980

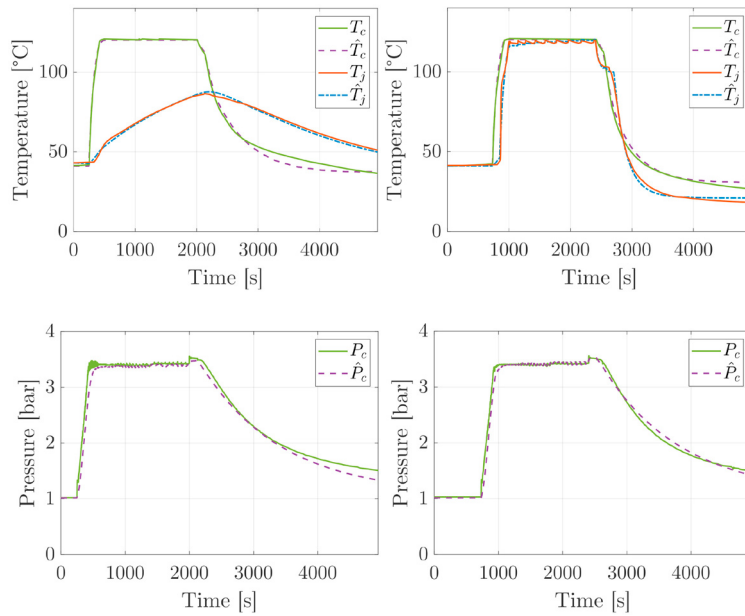


Fig. 2: Temperature (top) and pressure (bottom) profiles obtained during the cycle n. 7 (left) and 9 (right): reference values (green and red) are compared to the simulated ones (dotted purple and dotted blue).

The overall performance is satisfactory, with $\overline{FIT} = 94.26\%$ and $\overline{\rho} = 0.998$ for the temperature and $\overline{FIT} = 91.55\%$ and $\overline{\rho} = 0.998$ for the pressure. Contrarily to the results obtained in [6], no particular difference has been noticed with respect to the initial temperature, in fact only $k_{c,u_{2m}}$ required this differentiation. The validation results of the temperature in the jacket are reported in the same table. The model validation obtained great results with $\overline{FIT} = 90.45\%$ and $\overline{\rho} = 0.976$. An example is reported in Figure 2 where datasets 7 (left) and 9 (right) are shown. T_c and T_j (top) are the real temperatures in the chamber and in the jacket, P_c (bottom) is the real pressure in the chamber, while \hat{T}_c , \hat{T}_j and \hat{P}_c are the correspondent predictions.

Even if several physical aspects of the process have been neglected in the modelling procedure, the main behaviours of temperatures and pressure are satisfactorily represented as proved by high FIT values. With additional data coming from different machines, a portability study of this model could be carried out. In principle, the model is generic enough to be easily adapted modifying the ingoing/outgoing flow and the time delays typical of the considered datasets. Of course, the definition of the physical equation and the identification of the parameters are not trivial tasks but the quality reached is high enough to use this model as a reliable simulator for control design.

4. Neural network for control

The current FHA system is equipped with simple controllers, like PID, that do not require a model. Considering in particular the modulated valves described in Section 3.1, their behaviour can be further improved applying a more complex control approach such as model-based solutions. In this case, models with a lower complexity with respect to the one used in simulation are required to perform predictions. In the recent years, the growing diffusion of neural networks in many scientific fields has provided useful tools also for identification and control. Among the several neural networks architectures present in literature, Recurrent Neural Networks (RNNs) are considered in this work, since they have very good performances in terms of prediction but are also able to take into account the stability of the system as discussed in [10]. In this work a specific type of RNN, the Long Short-Term Memory (LSTM) network, proposed for the first time by [5], is considered.

4.1. LSTM description and training

The LSTM has a chain-like structure typical of the RNNs. The layer equations shown in the following are the ones described in [3]:

$$\begin{aligned} x^+ &= \sigma_g(W_f u + U_f \xi + b_f) \circ x + \sigma_g(W_i + U_i \xi + b_i) \circ \sigma_c(W_c u + U_c \xi + b_c) \\ \xi^+ &= \sigma_g(W_o u + U_o \xi + b_o) \circ \sigma_c(x^+) \\ y &= C \xi + b_y \end{aligned} \tag{9}$$

where $u \in \mathbb{R}^{n_u}$ is the input, $x \in \mathbb{R}^{n_x}$ the hidden state, $\xi \in \mathbb{R}^{n_x}$ the output state and $y \in \mathbb{R}^{n_y}$ the output of the system, while $\sigma_g = 1/(1 + \exp^{-x})$ and $\sigma_c = \tanh(x)$ are the activation functions, with $\sigma_g \in [0, 1]$ and $\sigma_c \in [-1, 1]$. The weights $W \in \mathbb{R}^{n_x \times n_u}$, $U \in \mathbb{R}^{n_x \times n_x}$ and $C \in \mathbb{R}^{n_u, 2n_x}$ and the biases b are the parameters to be defined during the training of the network.

The inputs are assumed bounded, with $u \in \mathcal{U} = [-1, 1]^{n_u}$ and this holds since are subjected to normalization techniques. Consequently, considering the activation functions bounds, also the output states is bounded, so $\xi \in \Xi = [-1, 1]^{n_x}$. Calling $\chi = [x^T \ \xi^T]^T$ and considering b_c as a constant input, the system (9) can be written as a non-linear dynamical system:

$$\begin{aligned} \chi^+ &= f_{LSTM}(\chi, u, b_c) \\ y &= g_{LSTM}(\chi) \end{aligned} \tag{10}$$

In [1] the stability properties of LSTM networks are investigated and a sufficient condition to guarantee the Input-to-State (ISS) stability of the network is provided.

Considering the definition of \mathcal{K} , \mathcal{K}_∞ and \mathcal{KL} functions in [7] and calling $\chi(k, \chi_0, \mathbf{u}, b_c)$ the state of the system (10) at time k with initial state χ_0 and input sequence $\mathbf{u} = (u(0), u(1), \dots)$, the following definitions and theorems are valid.

Definition 1 ([7]). *The system (10) is Input-to-state stable with respect to $u \in \mathcal{U}$ and b_c if there exist functions $\beta \in \mathcal{KL}$ and $\gamma_u, \gamma_b \in \mathcal{K}_\infty$ such that, for any $k \in \mathbb{Z}_{\geq 0}$, any initial condition χ_0 , any value of b_c and any input sequence $\mathbf{u} \in \mathcal{U}$, it holds that:*

$$\|\chi(k, \chi_0, \mathbf{u}, b_c)\|_2 \leq \beta(\|\chi_0\|_2, k) + \gamma_u(\|\mathbf{u}\|_\infty) + \gamma_b(\|b_c\|_2) \tag{11}$$

Definition 2 ([7]). *A continuous function $V : \mathbb{R}^n \rightarrow \mathbb{R}_+$ is called an ISS-Lyapunov function for (10) if there exist functions $\psi_1, \psi_2, \psi \in \mathcal{K}_\infty$ and $\sigma_u, \sigma_b \in \mathcal{K}$ such that for all $\chi \in \mathbb{R}^{2n_x}$, for all $b_c \in \mathbb{R}^{n_x}$ and $u \in \mathbb{R}^{n_u}$, it holds that:*

$$\begin{aligned} \psi_1(\|\chi\|_2) &\leq V(\chi) \leq \psi_2(\|\chi\|_2) \\ V(f_{LSTM}(\chi, u, b_c)) - V(\chi) &\leq -\psi_2(\|\chi\|_2) + \sigma_u(\|u\|_2) + \sigma_b(\|b_c\|_2) \end{aligned} \tag{12}$$

Theorem 1 ([7]). *If system (10) admits a time invariant ISS Lyapunov function such that (12) hold, then it is ISS in the sense specified in Definition 1.*

Theorem 2 ([1]). *Given the LSTM network (9), if*

$$\begin{aligned} (1 + \sigma_g(\|W_o \ U_o \ b_o\|_\infty)) \sigma_g(\|W_f \ U_f \ b_f\|_\infty) &< 1 \\ (1 + \sigma_g(\|W_o \ U_o \ b_o\|_\infty)) \sigma_g(\|W_i \ U_i \ b_i\|_\infty) |U_c| &< 1 \end{aligned} \tag{13}$$

then (9) is Input-to-State stable with respect to $u \in \mathcal{U}$ and to b_c .

Theorem 2 can be used to check the ISS property of the network a posteriori or to define constraints in the training phase to ensure the ISS property of the network. In this work, the second method was chosen, so the loss function J_{LSTM} used during the training phase has been modified, including Condition (13) as soft constraints as follows:

$$J_{LSTM} = \frac{1}{2L} \sum_{i=1}^L (\hat{Y}(i) - Y(i))^2 + \mu(\rho_1 A_1 + \rho_2 A_2) \quad (14)$$

considering

$$\begin{cases} A_1 = 0 & \text{if } \psi_1 < 1 \\ A_1 = (1 + \epsilon - \psi_1)^2 & \text{if } \psi_1 \geq 1 \end{cases} \quad \begin{cases} A_2 = 0 & \text{if } \psi_2 < 1 \\ A_2 = (1 + \epsilon - \psi_2)^2 & \text{if } \psi_2 \geq 1 \end{cases} \quad (15)$$

having fixed

$$\begin{aligned} \psi_1 &= (1 + \sigma_g(\|W_o U_o b_o\|_\infty)) \sigma_g(\|W_f U_f b_f\|_\infty) \\ \psi_2 &= (1 + \sigma_g(\|W_o U_o b_o\|_\infty)) \sigma_g(\|W_i U_i b_i\|_\infty) |U_c|_1 \end{aligned} \quad (16)$$

where L is the mini-batch size considered at each iteration, \hat{Y} is the prediction, Y the real data, μ , ρ_1 , ρ_2 and ϵ are parameters to be tuned.

The training has been performed using the Matlab environment, to obtain both temperature and pressure profiles in the chamber. The jacket temperature is not considered in the LSTM since it is not a variable of interest for the controller. The network was tuned considering 23 features, 300 hidden states and 600 epochs, considering a mini-batch size of 2. The Adam optimizer was used with initial learn rate $\alpha = 0.001$ (with 0.8 drop factor after 70 epochs), decay rate $\beta_1 = 0.9$ and squared decay rate $\beta_2 = 0.99$.

4.2. Results

Considering the 10 datasets listed in Table 2, the training was performed on half of the datasets and tested on the other half, as done before in Section 3.2 for the PhM. The results are shown in Table 3 (right), considering the performance indexes described in Section 3.3. Looking at the results, it can be observed that good performances are obtained for the first three datasets while the results are not satisfactory for datasets 9 and 10. From an analysis of the datasets characteristics reported in Table 2, it can be noticed that these datasets have some singular characteristics: dataset 9 uses both plates and jacket for auxiliary cooling with drain 2 and dataset 10 uses both plates and jacket for auxiliary heating. These particular combinations are present only in these two datasets, so the network is not able to recognize them during testing. A limitation of the LSTM approach is that the network is not able to deduce an unseen behaviour such as the PhM, so all the possible combination have to be inserted in the training dataset. A solution may consist in adding datasets 9 and 10 to the training set but not enough data will be then available for the testing. So, more datasets would be needed for a better training of the network, but the possibility of collecting these particular datasets is limited. For the moment, in first analysis, these two datasets are not considered. Hence, looking at the performances of datasets 1, 4 and 7, reported in Table 3, the overall performance is satisfactory with $\overline{FIT} = 84.586\%$ and $\bar{\rho} = 0.988$ for the temperature and $\overline{FIT} = 78.312\%$ and $\bar{\rho} = 0.98$ for the pressure. If the controller would have to manage cycles with features similar to the ones that generated dataset 9 and 10, an update of the network will be required.

5. Discussion

The goal of this work is the modelling of a complex process like the sterilization performed by an industrial autoclave, for both the simulation of the physical process and the development of an advanced model-based control like a Model Predictive Control (MPC). To do this, two ad-hoc models are developed: a physical model based on the physical knowledge of the process for simulation and a black-box one based on innovative machine learning techniques to obtain predictions necessary for the application of the advanced control system. Both the models obtain satisfactory results, considering their own specific target, highlighting at the same time their limitations.

The PhM gives excellent results but, requiring an accurate study of the physical transformations involved in the process, it's not trivial and requires a lot of time. It is a powerful tool to be used for simulation but does not fit well control requirements. On the other hand, the LSTM network provides satisfactory predictions and ensures ISS

properties. Anyway, as seen before, it is not able to predict behaviours not present in training datasets. Actually, the development of an MPC controller based on the neural network model is under study; since it is not a trivial task, it is proposed as future development.

6. Conclusions

In this work, two models for an industrial autoclave have been developed following two different approaches: a physical model, starting from a simpler one proposed in [6], and a black box model using a recurrent neural network. The PhM has been built considering new components with respect to [6] that imply several options for the heating and cooling of the chamber. Seen the high number of parameters involved in each phase, it is not possible to select portions of data where only a limited number of parameters contribute to the state evolution as in the previous work. The optimization problem is characterised by heavy computational load and a possible simplification to reduce it is currently under study. The results show a FIT of 94.26% for the temperature and of 91.55% for the pressure in the chamber. For what concerns the new components, the performance of the temperature in the jacket obtained a FIT of 90.45%. The black-box model was obtained through the training of a particular recurrent neural network, the LSTM ensuring ISS properties. The results show a FIT of 84,59% for the temperature and of 78,31% for the pressure in the chamber showing not negligible limitation for the representation of unseen behaviours. In summary, the physical model can be used to perform simulation and analyse the effect of components change even before the machine building, requiring time and effort to acquire the specific knowledge of the physical behaviour of the machine. The LSTM can be used for control applications. On the other hand, it does not reflect the physical composition of the machine and if a component is changed, a new training phase is required waiting the building of the new machine and the new data acquisition. Future developments of this work include an optimization procedure of the parameters for the PhM and the development of an MPC controller based on the LSTM network.

Acknowledgements

This work was supported by Fedegari Autoclavi SpA through the project entitled "Sviluppo di un tool di modellizzazione e simulazione dei gruppi di fasi (P/G) del controllore Fedegari per autoclavi".

References

- [1] Bonassi, F., Terzi, E., Farina, M., Scattolini, R., 2019. Lstm neural networks: Input to state stability and probabilistic safety verification. arXiv preprint arXiv:1912.04377.
- [2] Dorfling, C., Akdogan, G., Bradshaw, S., Eksteen, J., 2013. Modelling of an autoclave used for high pressure sulphuric acid/oxygen leaching of first stage leach residue. part 1: Model development. *Minerals Engineering* 53, 220 – 227.
- [3] Gers, F.A., Schmidhuber, E., 2001. Lstm recurrent networks learn simple context-free and context-sensitive languages. *IEEE Transactions on Neural Networks* 12, 1333–1340.
- [4] Green, D.W., 1973. Perry's chemical engineers' handbook/edición don w. Green y Robert H. Perry 100, 660–28.
- [5] Hochreiter, S., Schmidhuber, J., 1997. Long short-term memory. *Neural computation* 9, 1735–1780.
- [6] Iacono, F., Ferretti, S., Mezzadra, A., Magni, L., Toffanin, C., 2019. Industry 4.0: Mathematical model for monitoring sterilization processes - IEEE International Conference on Systems, Man, and Cybernetics.
- [7] Jiang, Z.P., Wang, Y., 2001. Input-to-state stability for discrete-time nonlinear systems. *Automatica* 37, 857–869.
- [8] Lau, W.L., Reizes, J., Timchenko, V., Kara, S., Kornfeld, B., 2015. Heat and mass transfer model to predict the operational performance of a steam sterilisation autoclave including products. *International Journal of Heat and Mass Transfer* 90, 800 – 811.
- [9] Ljung, L. (Ed.), 1999. *System Identification (2Nd Ed.): Theory for the User*. Prentice Hall PTR, Upper Saddle River, NJ, USA.
- [10] Mandic, D., Chambers, J., 2001. *Recurrent neural networks for prediction: learning algorithms, architectures and stability*. Wiley.
- [11] Pillai, V.K., Beris, A.N., Dhurjati, P.S., 1994. Implementation of model-based optimal temperature profiles for autoclave curing of composites using a knowledge-based system. *Industrial & Engineering Chemistry Research* 33, 2443–2452.
- [12] Pistolesi, D., Mascherpa, V., 2015. F0 a technical note URL: https://www.fedegari.com/wp-content/uploads/2019/03/ST19_EBook_F0-What-it-means-How-to-calculate-it-How-to-use-it.pdf.
- [13] Preglej, A., Karba, R., Steiner, I., Škrjanc, I., 2011. Mathematical model of an autoclave. *Strojniški vestnik-Journal of Mechanical Engineering* 57, 503–516.
- [14] Telikicherla, M., Altan, M., Lai, F., 1994. Autoclave curing of thermosetting composites: Process modeling for the cure assembly. *International Communications in Heat and Mass Transfer* 21, 785 – 797.